JOURNAL OF Materials CHEMISTRY

Equilibrium and non-equilibrium phase diagram within the TeO_2-rich part of the TeO_2–Nb_2O_5 system

Stéphanie Blanchandin, Philippe Thomas, Pascal Marchet, Jean Claude Champarnaud-Mesjard and Bernard Frit

Science des Procédés Céramiques et de Traitements de Surface, UMR 6638 CNRS, Université de Limoges, Faculté des Sciences, 123 avenue Albert-Thomas, 87060 Limoges Cedex, France

Received 29th January 1999, Accepted 18th May 1999

The TeO_2-rich part of the TeO_2–Nb_2O_5 system has been investigated by temperature programmed X-ray diffraction and differential scanning calorimetry. Three invariant equilibria have been observed: one eutectic reaction (8 mol% $NbO_{2.5}$, $T_E = 690 \pm 5$ °C, $L_E \rightleftharpoons TeO_2 + Nb_2Te_4O_{13}$), one peritectic reaction (incongruent melting, at 766 ± 5 °C, of the $Nb_2Te_4O_{13}$ compound) and one congruent melting reaction (congruent melting, at 810 ± 5 °C, of the $Nb_2Te_3O_{11}$ compound). A large glass-forming domain has been evidenced (0 to 25 mol% $NbO_{2.5}$). The thermal behaviour of these glasses has been followed. The glass transition, crystallization temperatures and the nature of crystalline phases formed have been determined.

Introduction

Tellurium dioxide-based glasses are very interesting materials for non-linear optical applications, especially optoelectronic devices (such as ultra-fast switching devices and optical transistors), because of their high linear and non-linear refractive indices and of their good visible and infrared light transmittance.[1–3] Numerous recent studies concerning these glasses have shown that their non-linear index n_2 was the highest found for oxide glasses and could be from 50 up to 100 times as large as that of SiO_2.[4–6] Accurate values of n_2 were measured at 1.5 μm for various tellurite glasses, using a time-resolved interferometric technique (n_2(Herasil) = $0.12(9) \times 10^{-19}$ m^2 W^{-1}; n_2(90% TeO_2–10% Nb_2O_5) = $6.9(7) \times 10^{-19}$ m^2 W^{-1}).[6] The origin of this non-linearity was attributed to the hyperpolarizability of the Te^{IV} lone pairs which is very often reinforced by addition of either a second lone pair holder (such as Tl^+, Bi^{3+}, Pb^{2+}) or of cations with empty d orbitals, such as Ti^{4+} or Nb^{5+}.[6–10] From this point of view, knowledge of the relationships between the structure and non-linear optical response of niobium tellurite glasses was of prime importance. So the TeO_2–Nb_2O_5 system was investigated. Previous studies concerning this system have revealed the existence of: (i) three crystalline phases, $Nb_2Te_4O_{13}$, $Nb_2Te_3O_{11}$ and Nb_6TeO_{17},[11–14] (ii) a large glassy domain whose composition range greatly differed from one study to another probably because of different experimental conditions (from 7 to 51 mol% $NbO_{2.5}$[15] and from 5 to 25 mol% $NbO_{2.5}$[16]). Investigations on the structure of these TeO_2–Nb_2O_5 glasses have shown that, with increasing Nb_2O_5 content, the TeO_4 structural entities observed in pure TeO_2 glass were progressively transformed into TeO_{3+1} units (three short bonds (Te–O < 2 Å) and one medium bond (Te–O ≈ 2.2–2.4 Å)).[8] However nothing is known about their thermal stability.

The aim of this study was both to determine the phase diagram under equilibrium and non-equilibrium conditions for the TeO_2-rich part of the TeO_2–Nb_2O_5 system and to follow the thermal behaviour of the glasses, *i.e.* their structural evolution with temperature and the determination of their phase transformation (T_t), glass transition (T_g), crystallization (T_c) and melting (T_l) temperatures.

Experimental

The crystallized samples were prepared by heating at 630 (for compositions ranging from 0 to 39 mol% $NbO_{2.5}$) or at 750 °C (for compositions ranging from 40 to 50 mol% $NbO_{2.5}$), in sealed gold tubes, intimate mixtures of commercial Nb_2O_5 (Aldrich, 99.5%) and TeO_2. The latter was prepared in the laboratory by decomposition at 550 °C of commercial H_6TeO_6 (Aldrich, 99.9%). Glassy samples were prepared by melting the same mixtures in platinum crucibles, for half an hour at 800 °C. The melts were quickly quenched by flattening between two brass blocks separated by a brass ring to obtain cylindrical samples 10 mm wide and 1.5 mm thick. In order to extend the glass forming range up to pure TeO_2 composition, samples containing 0 to 5 mol% $NbO_{2.5}$ were quenched using the method proposed by Kim *et al.*[5] The bottom of the platinum

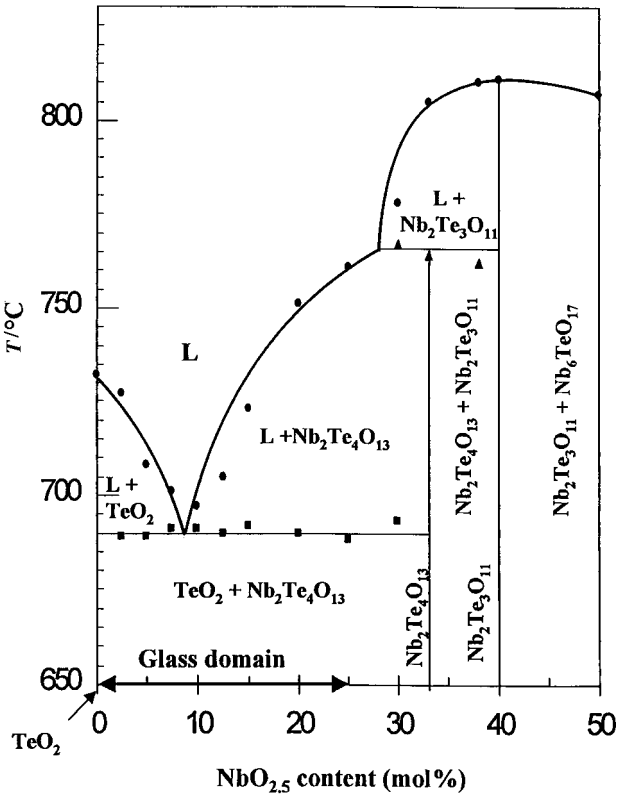

Fig. 1 Equilibrium phase diagram of the TeO_2-rich part of the TeO_2–$NbO_{2.5}$ system.

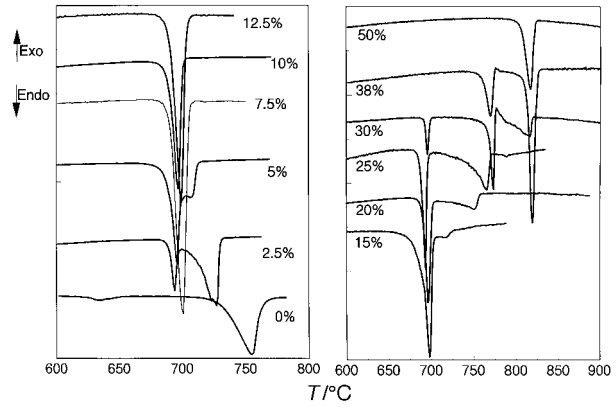

Fig. 2 DSC curves (solidus to liquidus part) of the $(1-x)TeO_2$–$xNbO_{2.5}$ samples ($0 \leqslant x \leqslant 0.50$) (heating rate 10 °C min^{-1}).

Table 1 XRPD data for $Nb_2Te_4O_{13}$

h,	*k,*	*l*	d_{obs}/Å	d_{calc}/Å	I/I_{max} (%)
0	2	0	10.67	10.75	1
1	1	−1	6.28	6.287	<1
1	1	1		6.276	
2	2	0	5.682	5.689	<1
0	4	0	5.368	5.375	1
2	0	−1	5.017	5.014	<1
2	0	1	5.003	5.003	<1
1	3	−1	4.839	4.845	<1
1	3	1		4.840	
2	2	−1	4.545	4.544	1
2	2	1	4.530	4.536	1
2	4	0	4.189	4.194	2
1	5	0	4.098	4.095	<1
3	3	−1	3.788	3.788	9
0	6	0	3.582	3.583	100
3	3	−1	3.395	3.390	7
3	3	1	3.381	3.385	5
4	0	0	3.351	3.352	21
2	0	−2	3.286	3.287	64
2	0	2	3.281	3.281	67
4	2	0	3.199	3.200	40
2	2	−2	3.146	3.144	21
2	2	2	3.142	3.138	18
0	4	2	3.086	3.085	3
4	0	−1	3.064	3.065	1
4	0	1	3.061	3.060	1
1	7	0	2.990	2.994	<1
4	2	−1	2.953	2.947	2
4	2	1	2.944	2.943	2
2	6	−1	2.921	2.916	<1
2	6	1	2.909	2.913	<1
3	5	−1	2.871	2.867	2
3	1	2	2.853	2.852	5
4	4	0	2.844	2.844	19
2	4	−2	2.809	2.804	12
2	4	2	2.803	2.801	13
1	7	−1	2.779	2.783	1
1	7	1		2.782	
3	3	−2	2.674	2.675	<1
3	3	2		2.670	
5	1	0	2.661	2.661	1
0	6	2	2.597	2.596	1
5	3	0	2.510	2.511	3
1	1	−3	2.454	2.453	2
1	1	3		2.451	
4	6	0	2.447	2.448	7
2	6	−2	2.421	2.422	49
2	6	2		2.420	
3	5	−2	2.392	2.395	2
3	5	2		2.391	
1	3	−3	2.337	2.335	3
1	3	3		2.333	
4	4	−2	2.270	2.272	3
4	4	2		2.268	

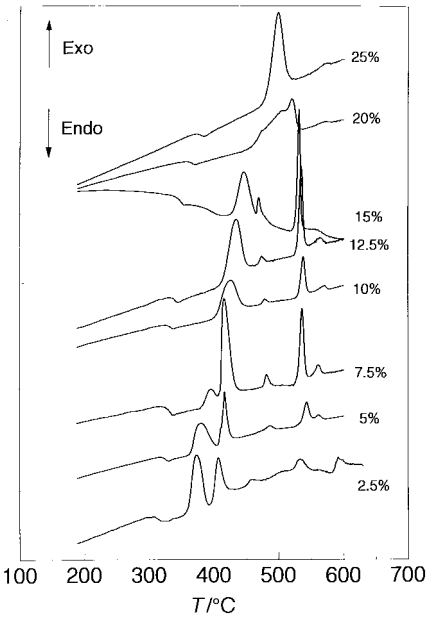

Fig. 3 DSC curves of the $(1-x)TeO_2$–$xNbO_{2.5}$ glasses ($0.025 \leqslant x \leqslant 0.25$) (heating rate 10 °C min^{-1}).

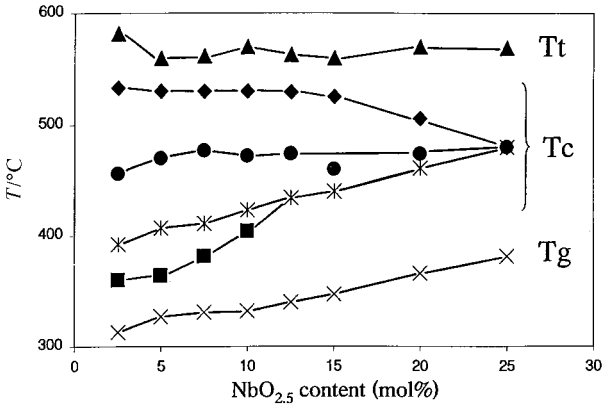

Fig. 4 Evolution with composition of the glass transition (x, T_g), crystallization (■, T_c: δ-TeO_2, ✳ γ-TeO_2, ● α-TeO_2, ◆ $Nb_2Te_4O_{13}$) and polymorphic transformation (▲, T_t: γ-TeO_2→α-TeO_2) temperatures of the TeO_2–$NbO_{2.5}$ glasses.

crucible was quickly dipped in a freezing mixture, consisting of ice, ethanol and NaCl kept at ≈ −11 °C.

Glass formation domain and crystallized phase compositions were determined by using X-ray diffraction (Guinier-De Wolff camera, Cu-Kα radiation). The structural evolution with temperature of glasses was followed by *in situ* X-ray powder diffraction (XRPD) with a Siemens D5000 diffractometer (θ/θ mode, Cu-Kα radiation) fitted with a high temperature furnace (Anton-Parr HTK10), a platinum heating sample holder and an Elphyse position sensitive detector (14° aperture). The heating rate was 5 °C min^{-1} and each XRPD pattern was recorded after an annealing time of 10 min at the chosen temperature, in the 2θ range 10–90° (step size 0.029, time range 18 min). Phase transformation, glass transition, crystallization and melting temperatures were measured by heat flux differential scanning calorimetry (DSC). A Netzsch STA 409 DSC instrument was used. The powdered samples (≈30 mg) were introduced into covered gold crucibles and the DSC curves were recorded between 20 and 800 °C using a heating rate of 10 °C min^{-1}. The glass transition temperature was taken as the inflection point of the steep change of the calorimetric signal associated with this transition. The crystallization temperature was taken as the intersection of the slope of the exothermic peak with the baseline. The liquidus

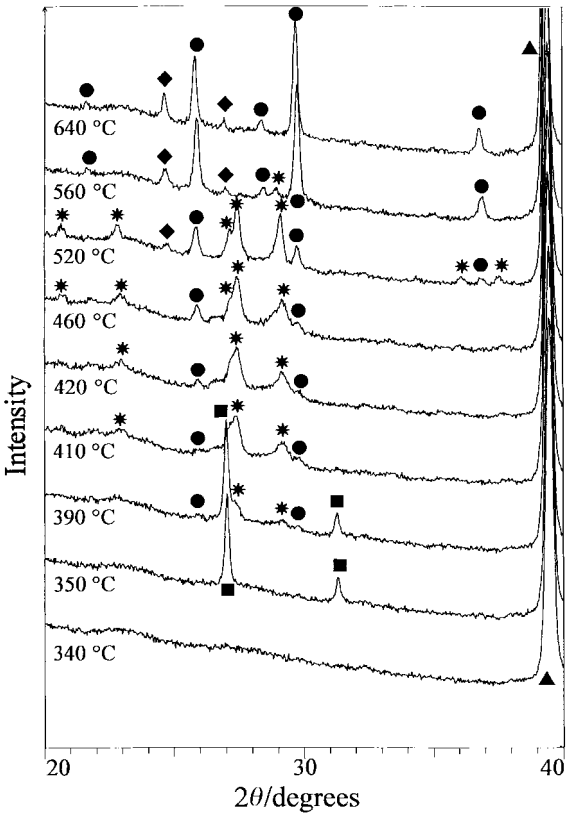

Fig. 5 XRD patterns at various temperatures of the 0.95 TeO_2–0.05 $NbO_{2.5}$ glassy sample (■ δ-TeO_2, ✳ γ-TeO_2, ● α-TeO_2, ◆ $Nb_2Te_4O_{13}$, ▲ Pt; Pt diffraction peaks are those of the sample holder).

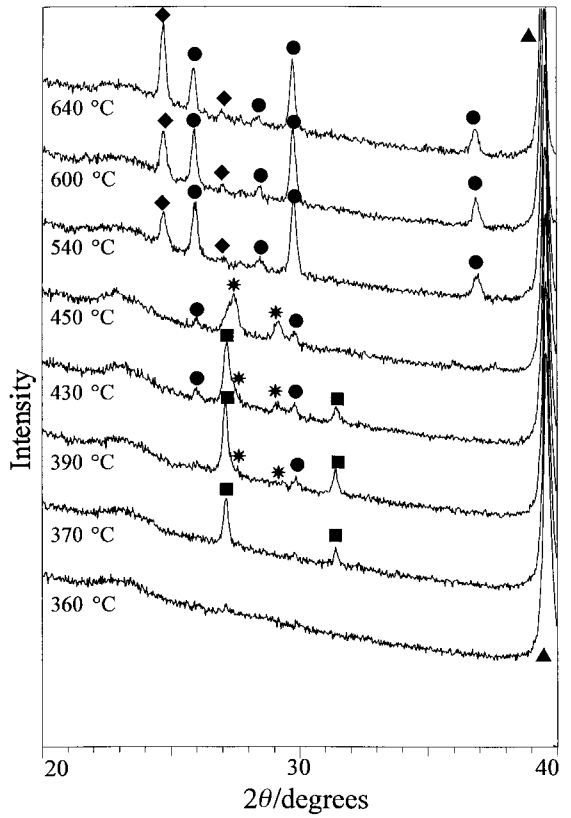

Fig. 6 XRD patterns at various temperatures of the 0.90 TeO_2–0.10 $NbO_{2.5}$ glassy sample (■ δ-TeO_2, ✳ γ-TeO_2, ● α-TeO_2, ◆ $Nb_2Te_4O_{13}$, ▲ Pt; Pt diffraction peaks are those of the sample holder).

temperature T_1 was considered to correspond to the bottom of the related endothermic peak. The energies of the different

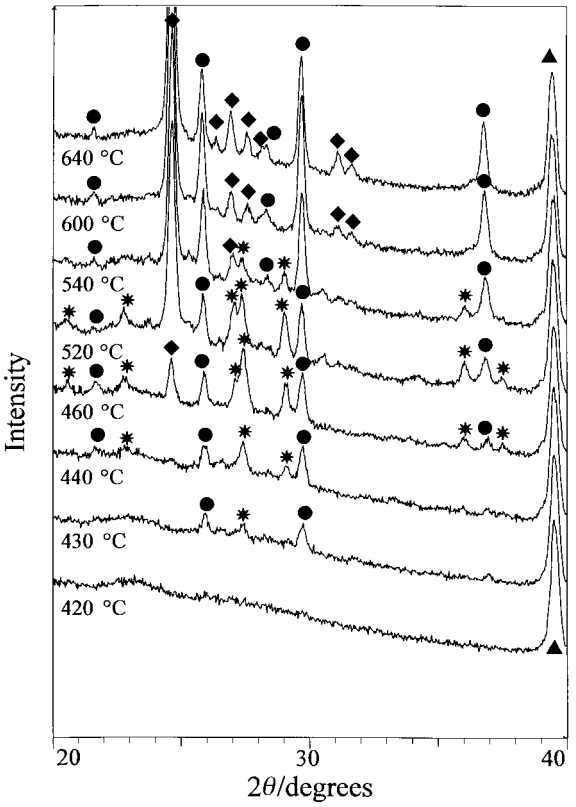

Fig. 7 XRD patterns at various temperatures of the 0.80 TeO_2–0.20 $NbO_{2.5}$ glassy sample (✳ γ-TeO_2, ● α-TeO_2, ◆ $Nb_2Te_4O_{13}$, ▲ Pt; Pt diffraction peaks are those of the sample holder).

thermal events were obtained from the areas under the corresponding peaks after heat-flow rate calibration (calibration substance: sapphire (100% pure Al_2O_3)).

The densities of both crystalline and glassy samples were measured on finely ground powders by helium pycnometry (Accupyc 1330 pycnometer).

Results and discussion

Equilibrium phase diagram

Our investigations within the TeO_2-rich part of the diagram have confirmed the existence in this composition range of the two crystalline phases previously evidenced: $Nb_2Te_4O_{13}$ and $Nb_2Te_3O_{11}$. The phase equilibrium diagram is shown in Fig. 1 and the corresponding DSC curves in Fig. 2. Three invariant equilibria have been detected: one eutectic reaction, one peritectic reaction and one congruent melting reaction.

The eutectic reaction (8 mol% $NbO_{2.5}$, $T_E = 690 \pm 5$ °C, $\Delta H_E = 25.9 \pm 0.5$ kJ mol^{-1}) corresponds to the equilibrium $L_E \rightleftharpoons TeO_2 + Nb_2Te_4O_{13}$. The peritectic reaction corresponds to the incongruent melting, at 766 ± 5 °C, of the $Nb_2Te_4O_{13}$ compound ($\Delta H_P = 12.7 \pm 0.5$ kJ mol^{-1}) and to the equilibrium $Nb_2Te_4O_{13} \rightleftharpoons L_P + Nb_2Te_3O_{11}$. The third equilibrium corresponds to the congruent melting at 810 ± 5 °C of the $Nb_2Te_3O_{11}$ compound ($\Delta H = 14.2 \pm 0.5$ kJ mol^{-1}). According to Galy and Lindqvist,[11] $Nb_2Te_3O_{11}$ crystallizes in space group $P2_12_12$ with $a = 7.700(2)$, $b = 15.700(3)$, $c = 3.980(1)$ Å, and $Z = 2$.

Single crystals of the $Nb_2Te_4O_{13}$ compound were obtained by heating an intimate mixture of 80 mol% TeO_2 and 20 mol% $NbO_{2.5}$ in a sealed gold tube at 800 °C for 12 h, and then slowly cooling it (2 °C min^{-1}) to 650 °C (30 h of annealing at this temperature). The crystallographic characteristics of this phase are: monoclinic symmetry (space group $C2/m$), $a = 13.409(5)$, $b = 21.503(6)$, $c = 7.534(4)$ Å, $\beta = 90.13(5)°$. The measured density ($\rho_{exp} = 5.48(5)$ g cm^{-3}) implies $Z = 8$ units

per cell ($\rho_{calc} = 5.53(2)$ g cm^{-3}). The corresponding indexed powder pattern is reported in Table 1.

Formation and thermal behaviour of glasses

Under our conventional conditions (melting at 800 °C and air-quenching), transparent and homogeneous yellowish glasses were obtained in the composition range 5 to 25 mol% $NbO_{2.5}$. The glass forming domain could be extended up to pure TeO_2 composition by quenching the melts in a mixture of ice, ethanol and NaCl. The densities regularly decrease from about 5.7 to 5.3 g cm^{-3} with increasing $NbO_{2.5}$ content, in agreement with previous studies.[2,7]

The DSC curves of the glassy samples are shown in Fig. 3. The evolution with composition of the glass transition and crystallization temperatures is reported in Fig. 4. T_g and T_c increase linearly with increasing $NbO_{2.5}$ content, *i.e.* with the decreasing amount of 'acidic' $Te^{IV}O_2$ and $(TeO_4)^{4-}$ structural entities as shown previously by Berthereau *et al.*[7,8] and Vogel.[15] The difference $T_g - T_c$, and so the thermal stability of glasses, increases with the $NbO_{2.5}$ content. The DSC peaks were unambiguously identified by the variable temperature XRD studies.

For pure TeO_2 glass, as we have previously reported,[17] the crystallization occurs with simultaneous formation of α-TeO_2 and of a new metastable γ-TeO_2 polymorph although the disappearance of the latter is observed above about 500 °C.

For samples in the range 2.5–12.5 mol% $NbO_{2.5}$ (see for example the XRD patterns at various temperatures of the sample with 5 mol% $NbO_{2.5}$ (Fig. 5)) five exothermic events are observed; first the crystallization of another metastable δ-TeO_2 polymorph, with cubic symmetry, previously observed in the TeO_2–WO_3 system.[17] The second peak is associated with the crystallization of γ-TeO_2 and the decomposition of the δ-TeO_2 form into the stable α-TeO_2 one. The third one corresponds to the crystallization of α-TeO_2, the fourth to crystallization of the $Nb_2Te_4O_{13}$ compound, and the last with the transformation of γ-TeO_2 into α-TeO_2. For the composition 90% TeO_2–10% $NbO_{2.5}$, crystallization of δ- and γ-TeO_2 occurs at nearly the same temperature so that only one large exothermic peak is observed on the DSC curve (Fig. 6).

For samples containing more than 10 mol% and up to 25 mol% $NbO_{2.5}$ (Fig. 7), the δ-TeO_2 phase is no longer observed and the four thermal events observed on the respective DSC curve are associated with the successive crystallizations of γ-TeO_2, α-TeO_2 and $Nb_2Te_4O_{13}$, and finally the transformation of γ-TeO_2 into α-TeO_2. These different thermal phenomena are observed more and more simultaneously with increasing $NbO_{2.5}$ content (Fig. 3 and 4). The transformation of γ-TeO_2 into α-TeO_2 is independent of the $NbO_{2.5}$ content and is observed at about 560 °C.

References

1 A. K. Yakhkind, *J. Am. Ceram. Soc.*, 1966, **49**, 670.
2 E. M. Vogel, M. J. Weber and D. M. Krol, *Phys. Chem. Glasses*, 1991, **32**, 231.
3 H. Takebe, S. Fujino and K. Morinaga, *J. Am. Ceram. Soc.*, 1994, **77**, 2455.
4 H. Nasu, T. Uchigaki, K. Kamiya, H. Kanbara and K. Kubodera, *Jpn. J. Appl. Phys.*, 1992, **31**, 3899.
5 S. H. Kim, T. Yoko and S. Sakka, *J. Am. Ceram. Soc.*, 1993, **76**, 1061.
6 B. Jeansannetas, S. Blanchandin, P. Thomas, P. Marchet, J. C. Champarnaud-Mesjard, T. Merle-Mejean, B. Frit, V. Nazabal, E. Fargin, G. Le Flem, M. O. Martin, B. Bousquet, L. Canioni, S. Le Boiteux, P. Segonds and L. Sarger, *J. Solid State Chem.*, in press.
7 A. Berthereau, Y. Le Luyer, R. Olazcuaga, G. Le Flem, M. Couzi, L. Canioni, P. Segonds, L. Sarger and L. Ducasse, *Mater. Res. Bull.*, 1994, **29**, 933.
8 A. Berthereau, E. Fargin, A. Villesuzanne, R. Olazcuaga, G. Le Flem and L. Ducasse, *J. Solid State Chem.*, 1996, **126**, 143.
9 J. C. Sabadel, P. Armand, D. Cachau-Hereillat, P. Baldeck, O. Doclot, A. Ibanez and E. Philippot, *J. Solid State Chem.*, 1997, **132**, 411.
10 B. Jeansannetas, Ph D Thesis, University of Limoges, 1998.
11 J. Galy and O. Lindqvist, *J. Solid State Chem.*, 1979, **27**, 279.
12 F. Garbassi, J. C. Bart and G. Petrini, *J. Electron Spectrosc. Relat. Phenom.*, 1981, **22**, 95.
13 O. Yamaguchi, T. Shirai, Y. Mukaida and K. Shimizu, *J. Chem. Soc., Dalton Trans.*, 1988, 2087.
14 V. V. Safonov and N. G. Chaban, *Russ. J. Inorg. Chem.*, 1994, **39**, 1147.
15 W. Vogel, *Glass Chemistry*, 2nd edn., Springer, Berlin, 1985.
16 H. G. Kim, T. Komatsu, R. Sato and K. Matusita, *J. Non-Cryst. Solids*, 1993, **162**, 201.
17 S. Blanchandin, P. Marchet, P. Thomas, J. C. Champarnaud-Mesjard, B. Frit and A. Chagraoui, *J. Mater. Sci.*, 1999, **34**, 1.

Paper 9/00788A